

Relative Attention-based One-Class Adversarial Autoencoder for Continuous Authentication of Smartphone Users

MINGMING HU, Institute of Information Engineering, Chinese Academy of Sciences, China
KUN ZHANG, Institute of Information Engineering, Chinese Academy of Sciences, China
RUIBANG YOU, Institute of Information Engineering, Chinese Academy of Sciences, China
BIBO TU*, Institute of Information Engineering, Chinese Academy of Sciences, China

Behavioral biometrics-based continuous authentication is a promising authentication scheme, which uses behavioral biometrics recorded by built-in sensors to authenticate smartphone users throughout the session. However, current continuous authentication methods suffer some limitations: 1) behavioral biometrics from impostors are needed to train continuous authentication models. Since the distribution of negative samples from diverse attackers are unknown, it is a difficult problem to solve in real-world scenarios; 2) most deep learning-based continuous authentication methods need to train two models to improve authentication performance. A deep learning model for deep feature extraction, and a machine learning-based classifier for classification; 3) weak capability of capturing users' behavioral patterns leads to poor authentication performance. To solve these issues, we propose a relative attention-based one-class adversarial autoencoder for continuous authentication of smartphone users. First, we propose a one-class adversarial autoencoder to learn latent representations of legitimate users' behavioral patterns, which is trained only with legitimate smartphone users' behavioral biometrics. Second, we present the relative attention layer to capture richer contextual semantic representation of users' behavioral patterns, which modifies the standard self-attention mechanism using convolution projection instead of linear projection to perform the attention maps. Experimental results demonstrate that we can achieve superior performance of 1.05% EER, 1.09% EER, and 1.08% EER with a high authentication frequency (0.7s) on three public datasets.

CCS Concepts: • **Security and privacy** → **Biometrics**; • **Human-centered computing** → **Collaborative and social computing**;

Additional Key Words and Phrases: Continuous authentication, Behavioral biometrics, Relative attention mechanism, One-class adversarial autoencoder.

ACM Reference Format:

Mingming Hu, Kun Zhang, Ruibang You, and Bibo Tu. 2022. Relative Attention-based One-Class Adversarial Autoencoder for Continuous Authentication of Smartphone Users. 1, 1 (November 2022), 23 pages. <https://doi.org/10.1145/nnnnnnn.nnnnnnn>

*Corresponding author

Authors' addresses: Mingming Hu, Institute of Information Engineering, Chinese Academy of Sciences, China, humingming0319@iie.ac.cn; Kun Zhang, Institute of Information Engineering, Chinese Academy of Sciences, China, zhangkun@iie.ac.cn; Ruibang You, Institute of Information Engineering, Chinese Academy of Sciences, China, youruibang@iie.ac.cn; Bibo Tu, Institute of Information Engineering, Chinese Academy of Sciences, China, tubibo@iie.ac.cn.

Permission to make digital or hard copies of part or all of this work for personal or classroom use is granted without fee provided that copies are not made or distributed for profit or commercial advantage and that copies bear this notice and the full citation on the first page. Copyrights for third-party components of this work must be honored. For all other uses, contact the owner/author(s).

© 2022 Copyright held by the owner/author(s).

XXXX-XXXX/2022/11-ART

<https://doi.org/10.1145/nnnnnnn.nnnnnnn>

1 INTRODUCTION

With the improvement of smartphones' processing power and storage capacity, smartphones have become an indispensable tool in our daily life. Smartphone users usually store a large amount of sensitive personal information and privacy information on their smartphones. Therefore, the leakage of personal privacy information on smartphones has aroused more and more people's concerns. Once personal privacy information is leaked, it will have a major negative impact on individuals and the public. To prevent the personal privacy information on the smartphone from being accessed and obtained by unauthorized users, an authentication method that can effectively authenticate users who access the smartphone becomes more critical. Although the current authentication methods can perform identity authentication when the user accesses the smartphone, such as PIN-based passwords, graphical passwords, fingerprint recognition, and face recognition, they only perform one-time authentication when smartphone users log in. Once the illegal user controls the smartphone after the smartphone is authenticated, privacy information is accessible and available until the smartphone is log out. Therefore, there is a great need for an authentication method to authenticate smartphone users throughout the session to enhance smartphone security.

Among various solutions, behavioral biometrics-based continuous authentication is a promising solution. It utilizes sensory data from built-in smartphone sensors to authenticate smartphone users, which can measure users' behavioral patterns when interacting with smartphones. Compared with typical one-time authentication methods, continuous authentication based on behavioral biometrics has the following advantages: 1) no additional hardware support is required to obtain biometric data that can represent user's behavioral patterns; 2) the acquisition of sensor data does not require root access privilege; 3) smartphone user does not need to participate in the authentication process; 4) it can authenticate the user's identity throughout the session.

Although the current methods based on traditional machine learning or deep learning have made some exciting progress, they still suffer some limitations. First, sensory data from impostors (negative samples) are needed to train the continuous authentication model (binary classification or multi-classification) [1, 6, 11, 12, 15, 21, 39, 47], since the distribution of negative training data from diverse attackers are unknown, it is a difficult problem to solve in a real-world scenario. Besides, sharing of other smartphone users' biometric data (negative samples) may lead to the leakage of biometric data. Abuhamad et al. [1] proposed an LSTM architecture to capture smartphone users' behavioral patterns from sensory data. When training the model, in addition to selecting the sensory data from the legitimate user as positive samples, and they also use sensory data from other users as impostors' biometric data. Li et al. [21] proposed a continuous authentication system based on two-stream convolutional neural network. In the training phase, the two-stream convolutional neural network model is trained as a multi-classification task. Thus continuous authentication task should be considered as one-class learning or novelty detection task, as [30, 32, 34]. However, these continuous authentication methods cannot extract deep features from behavioral biometrics that can characterize smartphone user's behavioral patterns, resulting in unsatisfactory authentication performance. Second, the continuous authentication methods they proposed require training two models [6, 21–23, 46], which require a significant amount of time and storage space consumption. Li et al. [22] employ a wasserstein generative adversarial network (CWGAN) to generate additional samples to augment the original training samples. In the training phase, they apply a convolutional neural network architecture to learning valuable deep features from sensor data, and the extracted deep features are feed to the one-class SVM to classify the current user as a legitimate user or an impostor. Centeno et al. [6] apply a siamese convolutional neural network to learn smartphone users' behavioral patterns from raw sensor data. Based on the extracted deep features, they choose the one-class SVM as the classifier. Third, the authentication model's weak capability of capturing

smartphone users' behavioral patterns from sensor data leads to unsatisfactory authentication performance [20, 30, 32, 34, 39, 44, 46, 47]. Shen et al. [30] construct 48 statistical features from each sensor to represent the smartphone user's behavioral patterns and authenticate his identity. Experimental results show that they can achieve a false rejection rate of 5.03%, and a false acceptance rate of 3.98%. Zhu et al. [46] proposed a hybrid deep learning method, which includes a CNN-based architecture for mixture feature extraction, and a SVM classifier for effective model training. Experimental results demonstrate that the proposed method can achieve 95.01% authentication accuracy on a real-world dataset.

To overcome the disadvantages of currently continuous authentication methods, we propose a relative attention-based one-class adversarial autoencoder architecture for continuous authentication of smartphone users. The proposed authentication architecture consists of four parts. First, we propose a one-class adversarial autoencoder to learn behavioral patterns of the legitimate user, which is trained only with the positive samples from the legitimate user in an unsupervised manner. Second, based on the latent representation from the encoder, a latent discriminator is applied to force latent representations of legitimate user's samples subject to spatial distribution uniformly. Third, a sample discriminator is trained to distinguish between the positive samples and the negative samples generated by the decoder with a prior distribution $\tilde{z} \in \mathbb{U}(-1, 1)$. Note that the role of the sample discriminator is to allow the autoencoder to reconstruct higher-quality positive samples during the training phase, rather than to classify the access user as a legitimate user or an impostor during the test phase. Fourth, we modify the standard self-attention mechanism using convolution projection instead of linear projection to conduct the query, key and value maps. Compared with the standard self-attention mechanism [37], the relative attention mechanism is more suitable for applications in the scenarios with limited computing power. Experimental results demonstrate that the effective stack of convolutional layer and the constructed relative attention layer can improve the model's capability of capturing contextual semantic information from behavioral biometrics. Besides, unlike recent approaches, training a one-class classifier to classify the access user as a legitimate user or an impostor, we apply a probabilistic method [27] to compute the probability that the reconstructed sample is generated from the distribution of legitimate user's samples. To verify the feasibility of the proposed relative attention-based one-class adversarial autoencoder architecture, we design a continuous authentication system based on the proposed relative attention-based one-class adversarial autoencoder, which consists of four modules: sensor data acquisition module, data preprocessing module, relative attention-based one-class adversarial autoencoder module, and continuous authentication module. Experimental results show that the designed continuous authentication system can achieve excellent performance of 1.05% EER, 1.09% EER and 1.08% EER on HMOG dataset, BrainRun dataset and IDNet dataset, respectively.

In summary, the contributions of the paper are as follows:

- We propose a relative attention-based one-class adversarial autoencoder architecture to model the behavioral patterns of legitimate users, which solves the problem that negative samples from attackers are not easy to obtain in a real-world scenario.
- We combine the constructed relative attention layers and convolutional layers to enhance the capability of capturing contextual semantic information from smartphone users' behavioral biometrics.
- We design a continuous authentication system to evaluate the proposed relative attention-based one-class adversarial autoencoder architecture. Comprehensive evaluations and comparative experiments are performed to verify the effectiveness and the superiority of the proposed relative attention-based one-class adversarial autoencoder architecture on three public datasets.

The remainder of this article is organized as follows. Section 2 reviews the related work. We propose a relative attention-based one-class adversarial autoencoder architecture in Section 3. We detail the designed continuous authentication system in Section 4. Detailed performance evaluation experiments are presented in Section 5. Finally, we discuss the limitation of our work in Section 6. We conclude this work in Section 7.

2 RELATED WORK

2.1 Behavioral Biometrics-based Continuous Authentication

Smartphones have a variety of built-in sensors, such as accelerometer, gyroscope, magnetometer, elevation, which can capture acceleration, angular velocity, orientation, and other information. Sensory data recorded by these sensors can measure the smartphone users' behavioral patterns when interacting with smartphones.

In recent years, behavioral biometrics-based continuous authentication has attracted the attention of many researchers, related researchers conducted the latest, comprehensive, extensive, and targeted investigations on continuous authentication based on behavioral biometrics [2, 35]. Behavioral biometrics are categorized into the following categories: touch gesture-based authentication [3, 9, 31, 43], gait-based authentication [12, 33, 48], keystroke-based authentication [8, 18, 36, 45], hand waving-based authentication [4, 34, 42], and multi-model fusion [1, 20, 22, 23, 30], etc. Shen et al. [31] analyzed the feasibility and applicability of smartphone users' touch-interaction behavior for continuous authentication on a real-world scenario dataset. Experimental results demonstrate that the touch behavior of smartphone user interacting with smartphones can well represent the user's unique behavioral patterns. Giorgi et al. [12] proposed a continuous authentication architecture based on walking gait behavior analysis, which uses a recurrent neural network model for the authentication phase. In the experiments, different user walking behaviors or a combination of them are used to analyze the impact of walking type on smartphone user authentication. Krishnamoorthy et al. [18] proposed a keystroke dynamics-based authentication scheme, which applies the support vector machine classifier to classify the access user as a legitimate user or an impostor. Besides, they employed minimum redundancy maximum relevance mRMR feature selection method to improve authentication performance. Sitová et al. [34] introduced a set of behavioral features (HMOG) for continuous authentication of smartphone users. The HMOG features can capture subtle micro-movement and orientation dynamics resulting when smartphone users interact with smartphones. To solve the problem of insufficient training samples or uneven sample distribution in continuous authentication of smartphone users based on behavioral biometrics. Li et al. [20] applied five data augmentation approaches of permutation, sampling, scaling, cropping, and jittering to create additional data on the training samples. An effective feature fusion scheme plays an important role in improving the performance of continuous authentication. Li et al. [23] proposed a lightweight convolutional neural network architecture to learn and extract valuable deep features from statistical features. Besides, they employed a balanced feature concatenation to fuse the extracted valuable features.

In this paper, we leverage sensory data from the accelerometer, gyroscope, and magnetometer to capture smartphone users' behavioral patterns when users interact with smartphones.

2.2 Self-attention Mechanism

The self-attention mechanism [37] has achieved great success in the field of natural language processing (NLP). Due to the effectiveness and scalability of the self-attention mechanism, multiple works explore the combination of self-attention mechanism and convolutional neural network architecture in computer vision tasks.

Recently, pure transformer models or models combined pure transformer and convolutional neural networks are presented for computer vision tasks. Vision Transformer (ViT) [10] is the first to apply a standard transformer [37] to perform image classification tasks. When pretrained on a large-scale dataset, the performance of the ViT even surpass state-of-the-art ConvNets. To solve the problems faced by the migration of the standard transformer from the domain of natural language processing to the computer vision, Liu et al. [25] presented a hierarchical transformer, which applies shifted windows to compute the latent representation. Carion et al. [5] proposed an encoder-decoder network for object detection (DETR), which applies the standard transformer to learn rich contextual semantic information. Inspired by DETR [5], Li et al. [19] applied an effective squeeze-and expansion transformer layers for medical image segmentation. Jiang et al. [17] built a generative adversarial network architecture without convolution layers, which only uses the standard transformer. Han et al. [13] presented a transformer in transformer (TNT) network for image recognition. The TNT applies an outer transformer to learn global dependencies, and employs an inner transformer to extract useful features from pixel level.

Although the pure transformer has been proven to improve the performance of traditional convolutional neural networks (CNN), it also brings huge computational overhead, especially at high-resolution input. Many works employ self-attention within limited region (e.g., 5×5 grid). Wang et al. [40] combined the self-attention mechanism and residual learning with training a very deep residual network. Ramachandran et al. [28] applied a stand alone self-attention block to replace the core building block of ResNet [14]. Wu et al. [41] applied a convolutional projection to replace the linear projection in the pure transformer module. Li et al. [24] proposed a contextual transformer block to strength the capability of learning rich contextual semantic information among neighbor keys.

Considering that the proposed continuous authentication system is deployed on smartphones, this article presents a relative attention layer, which applies convolutional layers to modify the standard self-attention mechanism [37]. Unlike some previous works that applied self-attention block to replace the convolutional layers or as an enhancement on top of the convolutions, this article learns richer contextual information from behavioral biometrics through the effective stacking of relative attention layers and convolutional layers.

3 ARCHITECTURE OF RELATIVE ATTENTION-BASED ONE-CLASS ADVERSARIAL AUTOENCODER

As shown in Figure 1, the proposed relative attention-based one-class adversarial autoencoder consists of four components: relative attention layer, a denoising autoencoder, latent space discriminator, and a sample discriminator. We describe each component below.

3.1 Relative Attention Layer

The original self-attention mechanism [37] aims to learn the dependency between a unit and the entire input sequence. The attention value for a unit can be computed as:

$$\text{AttWeight}(x, x) = f(K(x), Q(x)) \tag{1}$$

$$\text{Attention}(x) = \text{AttWeight}(x, x) \cdot V(x) \tag{2}$$

$$x_{\text{out}} = \text{MLP}(\text{Attention}(x)) \tag{3}$$

where the $\text{AttWeight}(x, x)$ is the attention matrix between each unit from the input sequence and the entire input sequence. The Q, K, V is the query, keys, values mapping, respectively, and the f is the softmax function. The x_{out} is the final output with the multi-layer perceptron (MLP) transformation.

Taking into account the computational overhead of the original self-attention mechanism [37]. In this article, for a 2D feature map, give a unit $x_{i,j}$, we compute the relative attention weight between $x_{i,j}$ and the neighborhood $x_{a,b}$ ($a, b \in \eta(i, j)$), where the $\eta(i, j)$ is a set of neighbors in a fixed domain with $x_{i,j}$ as the center, e.g., a $k \times k$ grid centered at (i, j) in a 2D feature map.

As shown in Figure 2, we apply convolutions projection to perform the query, key, value embeddings, respectively. Then the relative attention value for the $x_{i,j}$ is computed as follows:

$$y_{i,j} = \sum_{a,b \in \eta(i,j)} \frac{\exp(q_{i,j}^T k_{a,b})}{\sum_{m,n \in \eta(i,j)} \exp(q_{i,j}^T k_{m,n})} v_{a,b} \quad (4)$$

$$\begin{aligned} q_{i,j} &= W_Q x_{i,j} \\ k_{i,j} &= W_K x_{i,j} \\ v_{i,j} &= W_V x_{i,j} \end{aligned} \quad (5)$$

where the $y_{i,j} \in \mathbb{R}^{d_{out}}$ is the output at $x_{i,j}$, and $q_{i,j}, k_{i,j}, v_{i,j} \in \mathbb{R}^{d_{out}}$ are the intermediate value produced by $x_{i,j}$ and its neighborhoods $\eta(i, j)$. $W_Q, W_K, W_V \in \mathbb{R}^{d_{out} \times d_{in}}$ are learned transforms.

3.2 Denoising Autoencoder

We employ a denoising autoencoder [38] network to learn latent representation from input. Compared with the standard autoencoder, the denoising autoencoder add noise to the input, and attempts to reconstruct the input. The denoising autoencoder can reduce overfitting and make the trained encoder more robust, thereby enhancing the generalization ability of the denoising autoencoder. Besides, as shown in Figure 1a, unlike the prior denoising autoencoder architecture, we improve the representation learning capability and capacity of the model through the effective stacking of convolutional layers and relative attention layers. We expect the designed denoising autoencoder to be able to reconstructed samples as if they are drawn from the real distribution of the input.

The reconstruction loss for the denoising autoencoder can be defined as:

$$L_{rec} = \| x - f(g(x + n)) \|^2 \quad (6)$$

where x is the input, f is the Decoder, g is the Encoder, and $n \sim \mathcal{N}(0, 0.2)$.

3.3 Latent Space Discriminator

In order for the encoder to encode the inner class samples to the latent space representation z with distribution close to the prior distribution $\tilde{z} \in \mathbb{U}(-1, 1)$. As shown in Figure 1b, we apply a latent space discriminator to force latent space representations of inlier class samples to be distributed uniformly across the prior distribution. The latent space discriminator is applied to distinguish between the low-dimensional latent space representations of inlier class samples and the samples drawn from the prior distribution \tilde{z} . The adversarial loss of the latent space discriminator D_l can be formulated as:

$$L_{latent} = [\log D_l(\tilde{z})] + [\log(1 - D_l(g(x)))] \quad (7)$$

The weights of g are updated to minimize this objective and the D_l tries to maximize it. The ultimate goal is to expect the low-dimensional latent space representation of inlier class samples to be distributed following the prior distribution \tilde{z} .

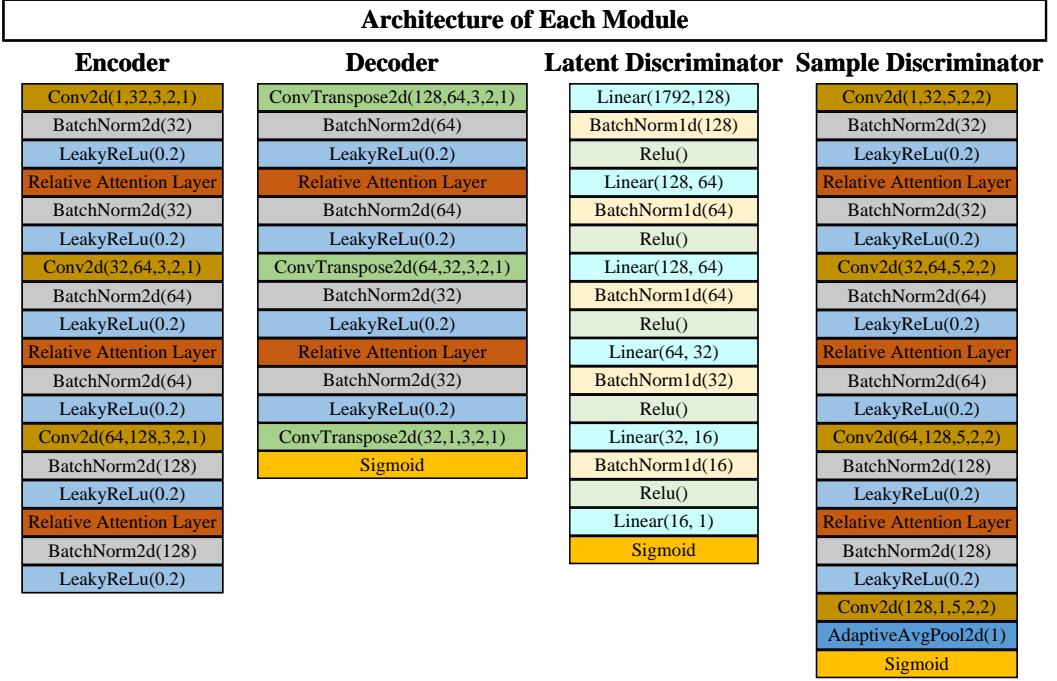


Fig. 3. Network architecture of the relative attention-based one-class adversarial autoencoder. Different layers are represented with different colors.

3.4 Sample Discriminator

A sample discriminator D_s is trained to distinguish between the positive samples and the negative samples generated from the decoder. The positive samples x are from the inlier class, and the negative samples $Decoder(\tilde{z})$ are generated by the decoder from the latent space with a prior distribution $\tilde{z} \in \mathbb{U}(-1, 1)$. As shown in Figure 1c, the sample discriminator architecture is composed of convolutional layers and relative attention layers. The decoder attempts to generate the negative samples that can fool the sample discriminator, and the sample discriminator learns to distinguish between the positive samples and the negative samples. The autoencoder and sample discriminator are trained as an adversarial game. We leverage the adversarial loss to improve the quality of reconstructed samples by autoencoder. The adversarial loss for the sample discriminator is formulated as:

$$L_{sample} = E [\log (D_s (x))] + E [\log (1 - D_s (Decoder(\tilde{z})))] \quad (8)$$

3.5 Implementation Details

Detailed network architecture of the relative attention-based one-class adversarial autoencoder is shown in Figure 3. The encoder contains three convolutional layer and three relative attention layers. For each convolutional layer and relative attention layer, followed by the batch normalization and the leaky Relu operations. The decoder consists of three transposed convolutional layers and two relative attention layers. These are, then followed by the batch normalization and the leaky Relu operations, except for the last transposed convolutional layer. A sigmoid activation operation

Algorithm 1: Training methodology of the relative attention-based one-class adversarial autoencoder. D_l and D_s represent the latent discriminator and the sample discriminator, respectively. En and De are the encoder and the decoder, respectively.

Input: Training set x , number of iterations N ,

Output: En, De, D_l , D_s

```

1 for iteration=1 to  $\rightarrow N$  do
2    $n \leftarrow \mathcal{N}(0, 0.2)$ 
3    $z \leftarrow \text{En}(x + n)$ 
4    $\tilde{z} \leftarrow \mathcal{U}(-1, 1)$ 
5   Sample discriminator update:
6    $L_{\text{sample}} \leftarrow D_s(\text{De}(\tilde{z}), 0) + D_s(x, 1)$ 
7   Back-propagate  $L_{\text{sample}}$  to update  $D_s$ 
8   Discriminator update:
9    $L_{\text{latent}} \leftarrow D_l(z, 0) + D_l(\tilde{z}, 1)$ 
10  Back-propagate  $L_{\text{latent}}$  to update  $D_l$ 
11
12  Autoencoder update:
13   $L_{\text{rec}} \leftarrow \|x - \text{De}(z)\|^2$ 
14   $L_{\text{sample}} \leftarrow D_s(\text{De}(\tilde{z}), 1) + D_s(x, 0)$ 
15   $L_{\text{latent}} \leftarrow D_l(z, 1) + D_l(\tilde{z}, 0)$ 
16  Back-propagate  $\lambda L_{\text{rec}} + L_{\text{sample}} + L_{\text{latent}}$  to update En, De

```

is applied after the last transposed convolutional layer. The latent discriminator contains six linear layers, and each linear layer is followed by the batch normalization and the Relu operations, except for the last linear layer. And, a sigmoid activation function is placed after the last linear layer. The sample discriminator contains four convolutional layers and three relative attention layers followed by the batch normalization and the leaky Relu operations, except for the last convolutional layer. An adaptive average pooling layer and a sigmoid activation function are placed after the last convolutional layer. The training step of the relative attention-based one-class adversarial autoencoder is summarized as Algorithm 1, and the λ is set to 10.

4 CONTINUOUS AUTHENTICATION SYSTEM

To evaluate the proposed relative attention-based one class adversarial autoencoder, we design and implement a comprehensive continuous authentication system. As shown in Figure 4, the proposed continuous authentication system is composed of three modules: 1) data acquisition module; 2) data preprocessing module; 3) continuous authentication module. We will describe the implementation of each module in detail.

4.1 Data Acquisition

When the user interacts with the smartphone, the sensory data collected by the smartphone's built-in sensors can imply the user's behavioral biometrics. The proposed continuous authentication system applies data collected from three sensors (accelerometer, gyroscope, magnetometer) to model smartphone user's behavioral patterns and then authenticate smartphone user's identity. The accelerometer is applied to measure the magnitude and direction of the acceleration of the

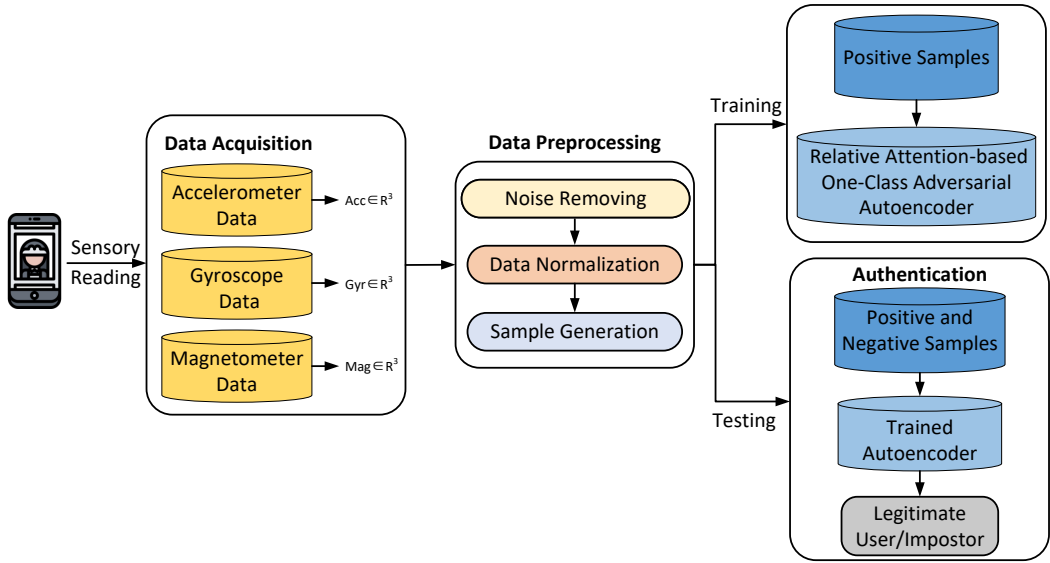


Fig. 4. Architecture of the proposed continuous authentication system.

smartphone due to force. It can record the movement patterns of smartphone user when interacting with smartphone. The gyroscope can measure the rotation rate of the smartphone when user interacts with smartphone. The magnetometer can measure the strength of the surrounding magnetic field and locate the location of the smartphone. The proposed continuous authentication system can learn smartphone users' behavioral patterns well by combining sensory data from three sensors.

4.2 Data Preprocessing

To enable the relative attention-based one-class adversarial autoencoder to learn rich contextual semantic information that can represent the legitimate user's behavioral patterns, we perform noise removing, data normalization, sample generation on the raw behavioral biometrics.

Noise Removing: The noise contained in sensor data reading make a significant impact on the authentication performance, which can be generated from sensor data collection stage. These noises may be generated by participants' irregular operations during sensor data collection. Therefore, noise should be removed to improve the sensor data readings' ability of characterizing smartphone user's behavioral patterns. There are two types of outliers that we will treat as noise: 1) signal mutation in smooth sensor signal, noise can cause some peaks in the smoothed sensor signal; 2) unchanged sensor signal for a period of time. During sensor data collection, participants may not interact with the phone for a period of time, for example, putting the smartphone on the desk.

Data Normalization: As shown in Figure 5, the biometric data collected by different sensors are significant difference in numerical values. If the biometric data are directly used as the input of the proposed relative attention-based one-class adversarial autoencoder, the deep learning model may highlight the role of larger values of biometric data, while relatively weakening the role of smaller values of biometric data. However, those biometric data with smaller values may play a decisive role in the final prediction results. Besides, the biometric data collected by multiple sensors may contain some noise and outliers. To reduce the large difference in biometric data distribution and

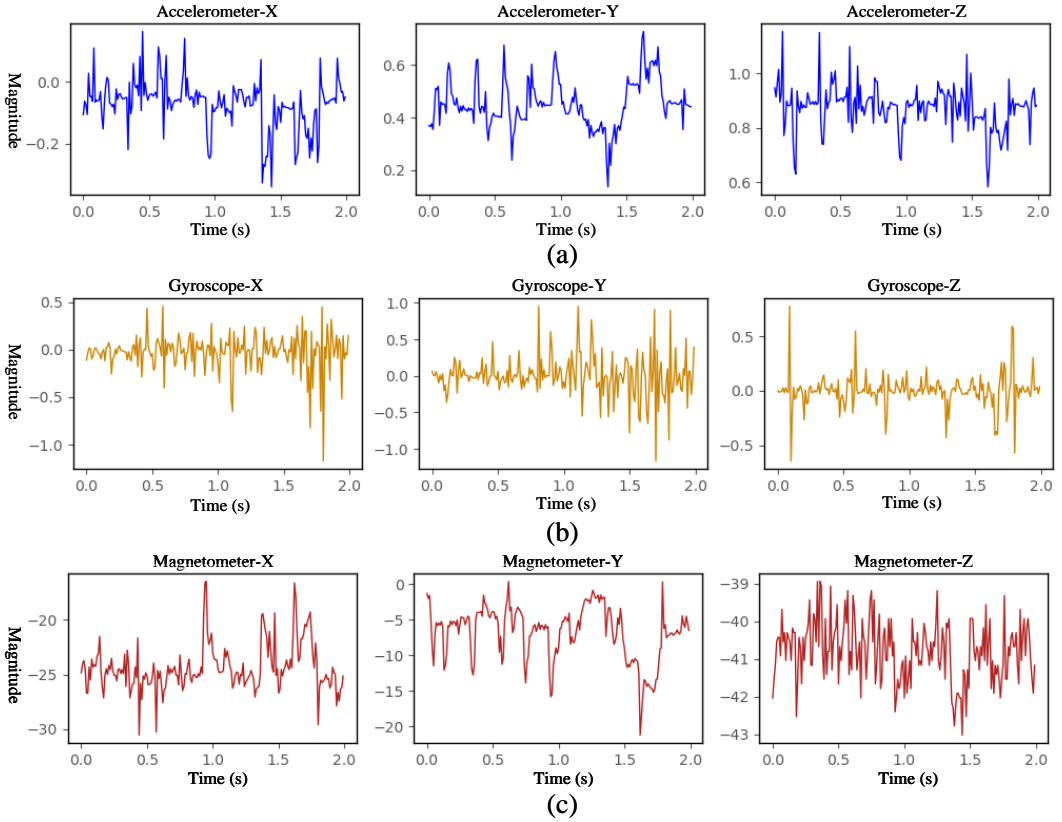


Fig. 5. The sensory readings of three-axis from different sensors. (a) sensory data sequence of three-axis from the accelerometer; (b) sensory data sequence of three-axis from the gyroscope; (c) sensory data sequence of three-axis from the magnetometer.

the influence of noise and outliers on the authentication performance, this article normalizes the biometric data from multiple sensors before fed to the relative attention-based one-class adversarial autoencoder.

In this article, min-max normalization is applied to perform a linear transformation on the raw biometric data. The biometric data sequence for each sensor in one axis can be represented as $(x_1, x_2, x_3, x_4, \dots, x_{n-1}, x_n) \in \mathbb{R}^n$, we perform normalization by:

$$y_i = \frac{x_i - \min_{1 \leq j \leq n} \{x_j\}}{\max_{1 \leq j \leq n} \{x_j\} - \min_{1 \leq j \leq n} \{x_j\}} \quad (9)$$

where the transformed biometric data for each sensor in one axis can be represented as $(y_1, y_2, y_3, y_4, \dots, y_{n-1}, y_n) \in [0, 1]$.

Sample Generation: Based on raw biometric data collected from multiple sensors (accelerometer, gyroscope, magnetometer), we need to process them into training samples for the input of the proposed relative attention-based one-class adversarial autoencoder. For each time point, the collected behavioral biometric data can be represented as $s = (x, y, z) \in \mathbb{R}^3$, where x, y, z is the three-axis of the sensory data. Besides, we also add a fourth axis for each sensor at

each time point, called Magnitude (M). The magnitude can be formulated as $M = \sqrt{x^2 + y^2 + z^2}$. Then for each time point, the behavioral biometric data from three sensors can be represented as $(x_{acc}, y_{acc}, z_{acc}, m_{acc}, x_{gyr}, y_{gyr}, z_{gyr}, m_{gyr}, x_{mag}, y_{mag}, z_{mag}, m_{mag}) \in \mathbb{R}^{12}$, where the acc, gyr, mag indicate the accelerometer, gyroscope, magnetometer, respectively. We apply a time window to segment the biometric data readings from three sensor without time overlap. Then for a time window t , the biometric data reading from three sensors can be represented as a $d \times n$ matrix:

$$S = \begin{bmatrix} x_{acc}^1 & x_{acc}^2 & \dots & x_{acc}^{n-1} & x_{acc}^n \\ y_{acc}^1 & y_{acc}^2 & \dots & y_{acc}^{n-1} & y_{acc}^n \\ z_{acc}^1 & z_{acc}^2 & \dots & z_{acc}^{n-1} & z_{acc}^n \\ m_{acc}^1 & m_{acc}^2 & \dots & m_{acc}^{n-1} & m_{acc}^n \\ x_{gyr}^1 & x_{gyr}^2 & \dots & x_{gyr}^{n-1} & x_{gyr}^n \\ y_{gyr}^1 & y_{gyr}^2 & \dots & y_{gyr}^{n-1} & y_{gyr}^n \\ z_{gyr}^1 & z_{gyr}^2 & \dots & z_{gyr}^{n-1} & z_{gyr}^n \\ m_{gyr}^1 & m_{gyr}^2 & \dots & m_{gyr}^{n-1} & m_{gyr}^n \\ x_{mag}^1 & x_{mag}^2 & \dots & x_{mag}^{n-1} & x_{mag}^n \\ y_{mag}^1 & y_{mag}^2 & \dots & y_{mag}^{n-1} & y_{mag}^n \\ z_{mag}^1 & z_{mag}^2 & \dots & z_{mag}^{n-1} & z_{mag}^n \\ m_{mag}^1 & m_{mag}^2 & \dots & m_{mag}^{n-1} & m_{mag}^n \end{bmatrix} \quad (10)$$

where the $d = 12$, and the $n = t * f$. We resample the biometric data readings with the sample rate $f = 100\text{Hz}$, and set the time window $t = 0.5\text{s}$. Then the training samples have a shape of 12×50 , which are fed to the relative attention-based one-class adversarial autoencoder for training.

4.3 Continuous Authentication Model

Unlike the current continuous authentication methods based on deep learning, which require impostors' behavioral biometric data (negative samples) to train the deep learning-based continuous authentication model. This article proposes a relative attention-based one-class adversarial autoencoder to continuously authenticate the smartphone user's identity, which does not require negative samples to train the model throughout the training phase. Therefore, the proposed continuous authentication model will not cause the leakage of smartphone users' behavioral biometric data. We have described the composition of relative attention-based one-class adversarial autoencoder in detail in Section 3.

In the authentication phase, we apply a probabilistic-based prediction approach to evaluate the reconstructed sample how likely it is generated by the distribution of the legitimate smartphone user's samples. Then we predict whether the test sample comes from a legitimate user or an impostor based on the calculated probability value. Give a sample $x \in \mathbb{R}^m$, it can be modeled as:

$$x = x^{\parallel} + \varepsilon = f(\tilde{z}) + \varepsilon = f(g(x)) + \varepsilon \quad (11)$$

where f is the decoder, g is the encoder. x can be non-linearly projected into $x^{\parallel} \in \mathcal{M}$. And $x^{\parallel} = f(\tilde{z})$ is low-dimensional manifold $\tilde{z} \in \mathbb{R}^n$ embedded to high-dimensional space with $m > n$, where $\tilde{z} = g(x)$. For the low-dimensional manifold \tilde{z} , linearization based on the first order Taylor expansion can be formulated as:

$$f(z) = f(\tilde{z}) + J_f(\tilde{z})(z - \tilde{z}) + o(\|z - \tilde{z}\|^2) \quad (12)$$

where J_f is the Jacobi matrix at point \tilde{z} . Defining Γ is the tangent space of f at \tilde{x} , the Γ is formulated as:

$$\Gamma = \text{span}(J_f(\tilde{z})) = \text{span}(U^\parallel S V^T) = \text{span}(U^\parallel) \quad (13)$$

where $U^\parallel S V^T$ is the SVD decomposition of the Jacobi matrix, and U is a unitary matrix. Then the sample x can be decomposed into two parts with the tangent space and the space orthogonal to it:

$$y = U^T x = \begin{bmatrix} U^{\parallel T} x \\ U^{\perp T} x \end{bmatrix} = \begin{bmatrix} y^\parallel \\ y^\perp \end{bmatrix} \quad (14)$$

where y^\parallel is parallel to Γ , and y^\perp is orthogonal to Γ , which is defined as a noise to make the sample x away from the manifold distribution \mathcal{M} . Then given a sample x , its probability prediction function $p_x(x)$ can be formulated as:

$$p_x(x) = p_y(U^T x) = p_y(y^\parallel, y^\perp) = p_{y^\parallel}(y^\parallel) * p_{y^\perp}(y^\perp) \quad (15)$$

Given a test sample $x \in \mathbb{R}^m$ and its non-linear projection $x^\parallel \in \mathcal{M} \subset \mathbb{R}^m$. It is assumed that $x \approx f(g(x))$, then the $p_{y^\parallel}(y^\parallel)$ can be formulated as:

$$\begin{aligned} p_{y^\parallel}(y^\parallel) &= p_{y^\parallel}(U^{\parallel T} x) = p_{y^\parallel}(U^{\parallel T}(x - x^\parallel) + U^{\parallel T} x^\parallel) \\ &= p_{y^\parallel}(U^{\parallel T}(x - f(g(x))) + U^{\parallel T} x^\parallel) \approx p_{y^\parallel}(U^{\parallel T} x^\parallel) \\ &= p_{x^\parallel}(x^\parallel) = p_{x^\parallel}(f(z)) = \det(USV^T)^{-1} * p_z(z) \\ &= \det S^{-1} * p_z(z) \end{aligned} \quad (16)$$

For each sample x , assuming that the noise is randomly distributed on the orthogonal manifold distribution. Then the intensity of noise y^\perp can be approximated by its distance to the center point of hypersphere S^{m-n-1} . Then the $p_{y^\perp}(y^\perp)$ can be formulated as:

$$p_{y^\perp}(y^\perp) \approx \frac{\Gamma(\frac{m-n}{2})}{2\pi^{\frac{m-n}{2}} \|y^\perp\|^{m-n}} p_{\|y^\perp\|}(\|y^\perp\|) \quad (17)$$

where the $\Gamma(\cdot)$ is the gamma function. The $p_{\|y^\perp\|}(\|y^\perp\|)$ can be learned offline by calculating the reconstruction error of the legitimate smartphone user's samples.

Given a sample x , if $p_x(x) \geq \tau$, the sample x is from the legitimate user, otherwise the sample x is from the impostor. The τ is a predefined threshold.

5 EXPERIMENTS

Comprehensive experiments are performed to verify the effectiveness and superiority of the proposed continuous authentication system based on a relative attention-based one-class adversarial autoencoder. The network architecture is implemented with the PyTorch library, and we train the network model on a Tesla T4 GPU for 100 epochs. The learning rate for the encoder, the decoder, the latent discriminator, and the sample discriminator are 0.00005, 0.0003, 0.00001, and 0.0001, respectively. The batch size is set to 16. Only the samples of legitimate user (positive samples) are needed to train the proposed relative attention-based one-class adversarial autoencoder during the training phase. We use 10 fold-cross-validation to train the continuous authentication model, and report the mean experimental results. We compute the AUROC, FAR, FRR, and EER with the TPR (True Positive Rate) equal to or greater than 97.0% in the experiments. The main goals of the evaluation experiments are as follows: 1) performance on different public datasets; 2) comparison with representative continuous authentication methods for the continuous authentication task; 3) the effectiveness of the relative attention layer in proposed one-class adversarial autoencoder

architecture; 4) performance with different time windows; 5) robustness against random attacks; 6) overhead Analysis.

5.1 Evaluation Metrics

Four evaluation metrics are used to evaluate the performance of the proposed continuous authentication system. The AUROC is the area under the Receiver Operating Characteristics (ROC) curve. The False Acceptance Rate (FAR) refers to the proportion of the number of times that illegitimate users are incorrectly authenticated as legitimate users to the total number of times that should be authenticated as the impostors, which can be formulated as $FAR = \frac{FP}{FP + TN}$. The False Rejection Rate (FRR) refers to the proportion of the number of times that legitimate users are incorrectly authenticated as the impostors to the total number of times that should be authenticated as legitimate users, formulating as $FRR = \frac{FN}{FN + TP}$. Equal Error Rate (EER) is defined as the point where the FAR equals the FRR. True Positive (TP) indicates the number of normal samples are correctly predicted as normal samples. False Positive (FP) indicates the number of anomalous samples are incorrectly predicted as normal samples. True Negative (TN) indicates the number of anomalous samples correctly are predicted as anomalous samples. False Negative (FN) indicates the number of normal samples are incorrectly predicted as anomalous samples.

5.2 Dataset

We evaluate the performance of the proposed continuous authentication system on three public dataset, which can be used for continuous authentication of smartphone users.

HMOG dataset: HMOG [34] is a new set of behavioral biometric data for continuous authentication of smartphone users, which contains the Hand Movement, Orientation, and Grasp (HMOG). The behavioral biometric data are collected from the embedded sensors (accelerometer, gyroscope, and magnetometer), when the user interacts with the smartphone. The dataset contains the behavioral biometric data of 100 participants (53 male and 47 female). For each participant, they collected an average of 1193 taps for each session and 1019 key presses. The average duration of collecting biometric data for each session is 11.6 minutes.

BrainRun dataset: BrainRun [26] applies a built-in gesture capture tool to capture different types of gestures in the sliding behavior of the user when interacting with the smartphone. The BrainRun dataset mainly contains three parts of behavioral biometric data. The gesture data contains the coordinate information of the screen points generated by each participant's tapping and swiping when interacting with the smartphone. The collected information includes the registered participants, the registered devices, and all the games played. The biometric data collected from the built-in sensors (accelerometer, gyroscope, magnetometer, and device motion sensor) from the smartphone. We use the raw behavioral biometric data collected from the embedded sensors (accelerometer, gyroscope, and magnetometer) of the smartphone. We randomly select 100 smartphone users' behavioral biometric data from the BrainRun dataset to perform the experiments.

IDNet dataset: IDNet dataset [16] is a gait data set from 50 participants, which is collected from inertial sensors (accelerometer, gyroscope, and magnetometer, etc.). Participants are asked to put their smartphones in the right front pocket of their trousers during sensor data collection phase. To bring the experimental scenarios closer to real world scenarios, participants are asked to walk as they felt comfortable during behavioral biometrics collection. We use the behavioral biometrics collected from three inertial sensors (accelerometer, gyroscope, magnetometer) to perform the experiments.

Table 1. The mean values of FAR (%), FRR (%), EER (%), and AUROC on different datasets.

Dataset	FAR ↓	FRR ↓	EER ↓	AUROC ↑
HMOG	0.77	1.39	1.05	0.998
BrainRun	0.99	2.05	1.09	0.997
IDNet	0.94	1.52	1.08	0.997

5.3 Performance on Different Public Datasets

To evaluate the performance of the proposed relative attention-based one-class adversarial autoencoder for the continuous authentication task, we perform several experiments on three public datasets. For each experiment, we randomly select one user from N users as the legitimate user and the rest $N-1$ as impostors. In the training phase, we randomly choose 80% samples of the legitimate user to train the relative attention-based one-class adversarial autoencoder. In the test phase, the rest 20% samples of the legitimate user and the whole samples of the impostors are used to test the trained authentication model. We train an authentication model for each smartphone user. Table 1 lists the mean FAR, FRR, EER, and AUROC of all smartphone users for each dataset. As shown in Table 1, the proposed relative attention-based one-class adversarial autoencoder achieves excellent performance on three public datasets. The proposed authentication method achieves 0.77% FAR, 1.39% FRR, 1.05% EER and 0.998 AUROC on the HMOG dataset, and 0.99% FAR, 2.05% FRR, 1.09% EER and 0.997 AUROC on the BrainRun dataset. It also reaches an average of 0.94% FAR, 1.52% FRR, 1.08% EER, and 0.997 AUROC on the IDNet dataset. Besides, to be able to observe the authentication performance of the proposed relative attention-based one-class adversarial autoencoder on single smartphone user, we also list the FAR, FRR, EER, and AUROC of ten randomly selected smartphone users from different public datasets in Table 2. As shown in Table 2, the proposed authentication method can achieve excellent FAR (less than 2.5%), FRR (less than 3%), EER (less than 2.5%), and AUROC (more than 0.990) on each random user.

5.4 Comparison with Representative Continuous Authentication Methods

Current continuous authentication methods are based on different datasets for performance evaluation. To make performance comparison experiments more convincing, we reproduce these authentication methods on three common datasets. Besides, we also make a qualitative comparison with representative work. The Acc., Gyr., Mag., To., Ori, El., and Gra. indicate the Accelerometer, Gyroscope, Magnetometer, Touch, Orientation, Elevation, and Gravity, respectively.

Performance comparison on three common datasets: We reproduce six representative continuous authentication methods on the HMOG dataset, BrainRun dataset, and IDNet dataset, including Roy et al. [29], Sitová et al. [34], Centeno et al. [6], Shen et al. [30], Li et al. [21], and Cherifi et al. [7]. Specially, Centeno et al. [6] and Li et al. [21] apply deep learning models to extract deep features from sensor data signals, and then traditional machine learning classifiers are used to classify the access user as the legitimate user or the impostor. Sitová et al. [34], and Shen et al. [30] construct multiple statistical features based on the sensor data signals, and apply the traditional machine learning classifiers to distinguish between the legitimate user and the impostor. We obtain the experimental settings from these articles. The traditional machine learning classification algorithms are from the scikit-learn library: one-class support vector machine (OC-SVM), hidden markov model (HMM). The deep metric learning model in [6] is implemented with the deep learning framework Keras, and the two-stream deep learning model in [21] is implemented with the PyTorch framework. Table 3 lists the Classifier, the training data, and the EER of representative work on

Table 2. The performance of ten randomly selected users from different public datasets.

Dataset	User ID	FAR ↓	FRR ↓	EER ↓	AUROC ↑
HMOG	100669	0.32	1.52	0.69	0.998
	180679	0.61	1.47	1.13	0.998
	220962	0.97	1.50	1.25	0.997
	352716	0.46	1.39	0.99	0.998
	525584	1.24	1.47	1.37	0.997
	553321	0.71	1.51	1.03	0.998
	622852	0.02	1.00	0.34	0.999
	745224	0.79	1.52	1.21	0.998
	799296	1.46	1.49	1.46	0.997
	962159	0.43	1.49	1.03	0.998
BrainRun	6jtbpdh	0.24	2.00	0.25	0.999
	8xjh8a	0.98	1.69	0.98	0.998
	9gx7uks	1.34	1.52	1.36	0.997
	gzx7rv	0.18	1.67	0.20	0.998
	sxvkh3b	0.86	1.67	0.88	0.998
	uui53he	1.09	2.56	1.28	0.997
	ioxyr9y	0.87	2.00	0.95	0.998
	w8f2wrs	0.97	1.81	1.10	0.998
	68n9ll	0.77	1.83	0.92	0.998
	d99p79w	2.32	2.60	2.32	0.992
IDNet	u002	0.89	1.15	0.96	0.998
	u004	1.65	1.60	1.61	0.996
	u008	1.55	1.89	1.55	0.997
	u012	1.35	1.61	1.48	0.997
	u013	0.49	1.58	0.79	0.998
	u024	0.18	1.19	0.31	0.999
	u029	0.89	1.72	0.93	0.998
	u041	0.86	1.32	0.88	0.998
	u043	1.47	1.66	1.47	0.997
	u046	1.29	1.55	1.29	0.997

Table 3. The EER (%) of representative continuous authentication methods on three datasets.

Work	Classifiers	Training data	Dataset		
			HMOG	BrainRun	IDNet
Roy et al. (2015) [29]	HMM	Owner	10.21	13.15	14.29
Sitová et al. (2016) [34]	Scaled Manhattan	Owner	16.34	18.64	19.07
Centeno et al. (2018) [6]	OC-SVM	Owner & Impostors	3.51	4.27	4.82
Shen et al. (2017) [30]	HMM	Owner	8.46	10.65	10.79
Li et al. (2020) [21]	OC-SVM	Owner & Impostor	5.85	7.21	7.93
Cherifi et al. (2021) [7]	HMM	Owner	15.49	17.86	18.31
Our work	Autoencoder	Owner	1.05	1.09	1.08

three common datasets. As shown in Table 3, the deep learning-based authentication methods achieve better authentication performance, including Centeno et al. [6], Li et al. [21], and our work. Among these representative authentication methods, our authentication approach achieve the best

Table 4. Qualitative comparison with representative continuous authentication methods.

Work	Sensors	Classifier	Training data	Results	Time (s)
Sitová et al. (2016) [34]	Acc., Gyr., Mag., To.	Scaled Manhattan	Owner	EER: 7.16% Walking	60
Centeno et al. (2018) [6]	Acc., Gyr., Mag.	OC-SVM	Owner & Impostor	Accuracy: 97.8%	>1
Shen et al. (2018) [30]	Acc., Gyr., Mag., Ori.	HMM	Owner	EER: 4.74%	8
Yang et al. (2019) [43]	To.	OC-SVM	Owner	Accuracy: 95.85%	0.01
Abuhamad et al. (2020) [1]	Acc., Gyr., Mag., To., El.	LSTM	Owner & Impostor	FAR: 0.96%, FRR: 8.08%	>0.5
Li et al. (2020) [21]	Acc., Gyr.	OC-SVM	Owner & Impostor	EER: 5.14%	3
Zhu et al. 2020 [47]	Acc., Gyr., Gra.	LSTM	Owner & Impostor	Accuracy: 91.59%	>3
Li et al. (2021) [22]	Acc., Gyr., Mag.	Isolation Forest	Owner & Impostor	EER: 3.64%	>2
Wang et al. (2021) [39]	Acc.	CNN	Owner & Impostor	Mcgill: 95.3% Accuracy	—
Shen et al. (2022) [32]	Acc., Gyr., Mag., To.	DeSVDD	Owner	EER: 14.9%	—
Our work	Acc., Gyr., Mag.	Autoencoder	Owner	HMOG: 1.05% EER	0.7

EER with 1.05%, 1.09%, and 1.08% on three datasets, respectively. More importantly, we only use the behavioral biometrics of the legitimate user to train the authentication model.

Qualitative comparison with representative continuous authentication work: We also make a qualitative comparison with representative continuous authentication work, including Sitová et al. [34], Centeno et al. [6], Shen et al. [30], Yang et al. [43], Abuhamad et al. [1], Li et al. [21], Zhu et al. [47], Li et al. [22], Wang et al. [39], and Shen et al. [32]. Table 4 lists the sensors, classifiers, training data, experimental result, and time overhead of each representative work. Sitová et al. [34] introduced a public dataset of smartphone users’ behavioral biometric features for the continuous authentication task. Experimental results shown that they can achieve the best authentication performance (7.16% EER in walking and 10.05% in sitting) when they fuse HMOG, taps, and keystroke features. Centeno et al. [6] apply a siamese convolutional neural network to extract deep features from sensor data signals, and they achieve 97.8% accuracy on the HMOG dataset using the one-class SVM classifier. Shen et al. [30] explored the contribution of each motion sensor behavior for the continuous authentication performance. Experimental results shown that they achieve the lowest EER of 4.74% when they combine the accelerometer, gyroscope, magnetometer, and orientation sensors. Yang et al. [43] explored the continuous authentication performance of different type of screen touch operations, including click operations and sliding operations. Abuhamad et al. [1] proposed an LSTM-based end-to-end continuous authentication approach, and explored different LSTM architectures in learning and capturing the behavioral patterns of smartphone users. Experimental results shown that they can achieve 0.96% FAR and 8.08% FRR using readings of only three sensors. Li et al. [21] utilize a two-stream convolutional neural network architecture to extract deep features from behavioral biometrics, and the OC-SVM classifier is used to classify the access user as a legitimate user or an impostor. Experimental results shown that the proposed authentication method can achieve an mean EER of 5.14% with approximately 3s authentication time. Zhu et al. [47] applied an optimized LSTM architecture to learn the behavioral patterns from three built-in sensors. Besides, they evaluated the performance of the proposed continuous authentication method on a large-scale real-world noisy dataset. Li et al. [22] apply a conditional wasserstein generative adversarial network to generate additional sensor data signals for data augmentation, and a convolutional neural network architecture is used to extract deep features from sensor data signals. Experimental results shown that they achieve the lowest EER of 3.64% using three motion sensors. Wang et al. [39] proposed a deep metric learning-based continuous authentication framework for smartphone users, which can be trained on the battery-powered smartphone. Experimental results demonstrate that they achieve authentication accuracy over 95% using only one motion sensor. Shen et al. [32] constructed a smartphone users’ behavioral biometrics dataset for the continuous authentication task, which are collected based

Table 5. Ablation study of the proposed relative attention-based one-class adversarial autoencoder on three datasets.

Architecture	Dataset	FAR ↓	FRR ↓	EER ↓
Without two discriminators and relative attention layer	HMOG	4.37	2.81	3.58
	BrainRun	4.64	2.97	3.83
	IDNet	4.76	2.85	3.79
With relative attention layer	HMOG	1.69	2.22	1.83
	BrainRun	1.85	2.45	1.91
	IDNet	1.92	2.31	1.88
With two discriminators	HMOG	2.98	2.55	2.74
	BrainRun	3.23	2.71	2.98
	IDNet	3.37	2.65	2.84
Two discriminators + relative attention layer	HMOG	0.77	1.39	1.05
	BrainRun	0.99	2.05	1.09
	IDNet	0.94	1.52	1.08

on unconstrained touch operations from 100 volunteers. Experimental results demonstrate that they can achieve 14.9% EER using a deep learning based one-class classifier (DeSVDD) on their dataset. Different from these representative work, we propose a relative attention-based one-class adversarial autoencoder to authenticate the smartphone user, which can achieve 1.05% EER with a high authentication frequency (0.7s) on the HMOG dataset.

5.5 Ablation Study

In order to evaluate the effectiveness of each part (relative attention layer, and two discriminators) in proposed one-class adversarial autoencoder architecture, we carry ablation study on three datasets (HMOG dataset, BrainRun dataset, and IDNet dataset). We remove the relative attention layer, and two discriminators from the proposed one-class adversarial autoencoder architecture, and perform authentication performance evaluation experiments on three datasets, respectively. Table 5 lists the mean experimental results without each part on three datasets. As shown in Table 5, the relative attention layer play an important role in improving authentication performance, the authentication performance of EER improves further by 1.5% with the relative attention layers. Experimental results demonstrate that we can further improve the authentication performance through the effective stacking of convolutional layers and relative attention layers. Besides, when the two discriminators are added, the authentication performance of EER is improved further by a 0.8% on three public datasets.

5.6 Performance with Different Time Windows

To evaluate the authentication performance with different time window size of behavioral biometrics sequences, we perform several experiments with different time window size on the HMOG dataset. Figure 6 shows the trend of the FAR, FRR, EER, and AUROC with the increase of time window size. The FAR in Figure 6a decreases with the increase of time window size from 0.25s to 0.5s, and then fluctuates slightly with the increase of time window size from 0.5s to 1.5s. The FRR and EER in Figure 6b and Figure 6c show the trend to the FAR. The AUROC in Figure 6d increases with the increase of time window size from 0.25s to 0.5s, and then keeps stable with the increase of time

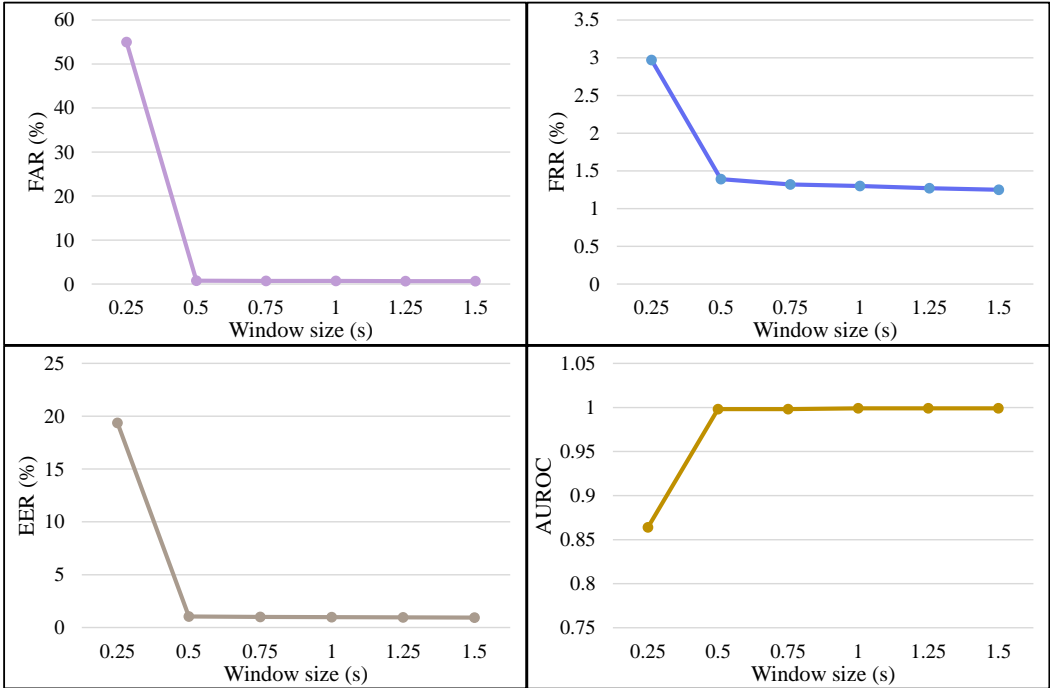


Fig. 6. The trend of the FAR, FRR, EER, and AUROC with the increase of time window size.

Table 6. The mean values of FAR (%), FRR (%), EER (%), and AUROC with different time window size.

Window size (s)	FAR ↓	FRR ↓	EER ↓	AUROC ↑
0.25	54.97	2.97	19.36	0.864
0.5	0.77	1.39	1.05	0.998
0.75	0.72	1.32	1.01	0.998
1	0.69	1.30	0.98	0.999
1.25	0.68	1.27	0.96	0.999
1.5	0.65	1.25	0.94	0.999

window size from 0.5s to 1.5s. Table 6 lists the mean values of the FAR, FRR, EER, and AUROC with different time window size. As shown in Table 6, we achieve excellent performance with the increase of time window size from 0.5s to 1.5s. Considering the time cost and authentication efficiency, we choose a 0.5s time window size of behavioral biometrics sequences in the experiments.

5.7 Robustness against Random Attacks

Random attack means that the attacker attempts to attack the legitimate user’s smartphone with his behavioral habit, he has no knowledge of the legitimate user’s behavioral patterns before attacking. In the experiments, similar to Wang et al. [39], we choose the smartphone user from HMOG dataset as the legitimate user, and the smartphone users from the BrainRun and IDNet dataset as attackers. Since different datasets are the behavioral biometrics of smartphone users collected under different scenarios, they can be used to simulate random attacks by multi-attackers.

Table 7. The mean values of FAR (%), FRR (%), EER (%), and AUROC under random attacks.

Attacker	FAR ↓	FRR ↓	EER ↓	AUROC ↑
BrainRun	0.01	1.41	1.28	0.996
IDNet	0.01	1.35	1.23	0.997

For each experiment, we randomly choose one smartphone user’s behavioral biometrics from HMOG dataset (100 users) to train the relative attention-based one-class adversarial autoencoder, and the behavioral biometrics from the BrainRun and IDNet dataset are used to launch attacks. We perform random attacks analysis on each smartphone user in the HMOG dataset (100 users). Table 7 lists the mean values of FAR, FRR, EER, and AUROC under random attacks. As shown in Table 7, the proposed authentication method can achieve 0.01% FAR, 1.41% FRR, 1.28% EER, 0.996 AUROC, and 0.01% FAR, 1.35% FRR, 1.23% EER, 0.997 AUROC under the random attacks from the BrainRun dataset and IDNet dataset, respectively. Experimental results demonstrate that the proposed continuous authentication approach can well resist the random attacks from diverse attackers.

5.8 Overhead Analysis

We evaluate the resource consumption of the proposed relative attention-based one-class adversarial autoencoder for continuous authentication of smartphone users in three aspects, including time efficiency, storage, and model parameter size and FLOPs.

Time efficiency: The time cost of the proposed continuous authentication method consists of three parts, including a certain time window of sensor data sequence for the authentication (t_1), the time of data preprocessing (t_2), and the time of the proposed relative attention-based one-class adversarial autoencoder for authentication (t_3). In the experiments, we choose a 0.5s time window of sensor data sequence for the authentication ($t_1=0.5s$). The time of data preprocessing is 130ms ($t_2=130ms$), including noise removing, data normalization, and sample generation. The time of the proposed relative attention-based one-class adversarial autoencoder for the authentication is 100ms ($t_3=100ms$). Then the total time cost is approximately 0.7s ($t_1+t_2+t_3$).

Storage: The pretrained relative attention-based one-class adversarial autoencoder consists of four parts, including the encoder, the decoder, the latent space discriminator, and the sample discriminator. The encoder and decoder have size of 650.9KB and 574.6KB, respectively. The latent space discriminator and sample discriminator have size of 970.1KB and 630.8KB, respectively. Then the total size of the proposed relative attention-based one-class adversarial autoencoder is 2.7MB.

Model parameter size and FLOPs: The encoder has 0.15M parameters and 0.01G FLOPs. The decoder has 0.1M parameters and 0.01G FLOPs. The latent space discriminator has 0.23M parameters and 0G FLOPs. The sample discriminator has 0.15M parameters and 0.09G FLOPs. Then the proposed relative attention-based one-class adversarial autoencoder has 0.63M parameters and 0.11G FLOPs in total.

6 DISCUSSION

We will discuss the limitation of our work in this section.

6.1 Limited Comparison with Representative Work on the Generic Dataset

The lack of a generic dataset as a benchmark to evaluate the performance of continuous authentication methods has been a limitation for behavioral biometrics-based continuous authentication

of smartphone users. Most researchers evaluated their behavioral biometrics-based continuous authentication approaches on their own datasets. For a fair performance evaluation comparison, as shown in Table 3, we reproduce six representative continuous authentication approaches on three public datasets. Besides, due to the lack of technical details and detailed implementation steps of some representative authentication methods, we cannot reproduce them, we can only make a qualitative comparison with some representative continuous authentication methods in Table 4. Lack of a fair performance comparison on the generic dataset is also a common problem with current behavioral biometrics-based authentication methods.

7 CONCLUSION

In this work, we propose a relative attention-based one-class adversarial autoencoder for continuous authentication of smartphone users. We combine the convolutional layers and the constructed relative attention layers to capture rich contextual semantic representation of smartphone user's behavioral patterns. More importantly, the proposed relative attention-based one-class adversarial autoencoder only learns the latent representations of legitimate user's behavioral patterns, which is trained without negative samples from impostors. The proposed authentication method achieves excellent performance with a high authentication frequency (0.7s) on three public dataset. Experimental results show that the proposed authentication method achieves 0.77% FAR, 1.39% FRR, 1.05% EER and 0.998 AUROC on the HMOG dataset. We also achieve excellent performance with 0.99% FAR, 2.05% FRR, 1.09% EER and 0.997 AUROC on the BrainRun dataset, and 0.94% FAR, 1.52% FRR, 1.08% EER and 0.997 AUROC on the IDNet dataset. Compared with representative continuous authentication methods, experimental results demonstrate that the proposed authentication method can achieve superior authentication performance. Besides, experimental results show that the proposed authentication method can achieve 0.01% FAR, 1.41% FRR, 1.28% EER, 0.996 AUROC, and 0.01% FAR, 1.35% FRR, 1.23% EER, 0.997 AUROC, when the behavioral biometrics from BrainRun dataset and IDNet dataset are used to launch the random attacks, respectively.

REFERENCES

- [1] Mohammed Abuhamad, Tamer Abuhmed, David Mohaisen, and DaeHun Nyang. 2020. AUToSen: Deep-learning-based implicit continuous authentication using smartphone sensors. *IEEE Internet of Things Journal* 7, 6 (2020), 5008–5020.
- [2] Mohammed Abuhamad, Ahmed Abusnaina, DaeHun Nyang, and David Mohaisen. 2020. Sensor-based continuous authentication of smartphones' users using behavioral biometrics: A contemporary survey. *IEEE Internet of Things Journal* 8, 1 (2020), 65–84.
- [3] Mohammed A Alqarni, Sajjad Hussain Chauhdary, Maryam Naseer Malik, Muhammad Ehatisham-ul Haq, and Muhammad Awais Azam. 2020. Identifying smartphone users based on how they interact with their phones. *Human-centric Computing and Information Sciences* 10, 1 (2020), 1–14.
- [4] Attallah Buriro, Bruno Crispo, and Yury Zhauniarovich. 2017. Please hold on: Unobtrusive user authentication using smartphone's built-in sensors. In *2017 IEEE International Conference on Identity, Security and Behavior Analysis (ISBA)*. IEEE, 1–8.
- [5] Nicolas Carion, Francisco Massa, Gabriel Synnaeve, Nicolas Usunier, Alexander Kirillov, and Sergey Zagoruyko. 2020. End-to-end object detection with transformers. In *European conference on computer vision*. Springer, 213–229.
- [6] Mario Parraño Centeno, Yu Guan, and Aad van Moorsel. 2018. Mobile based continuous authentication using deep features. In *Proceedings of the 2nd International Workshop on Embedded and Mobile Deep Learning*. 19–24.
- [7] Ferial Cherifi, Mawloud Omar, and Kamal Amroun. 2021. An efficient biometric-based continuous authentication scheme with HMM prehensile movements modeling. *Journal of information security and applications* 57 (2021), 102739.
- [8] D. Cilia and F. Inguanez. 2018. Multi-Model authentication using keystroke dynamics for Smartphones. In *2018 IEEE 8th International Conference on Consumer Electronics - Berlin*.
- [9] Quentin Debard, Christian Wolf, Stephane Canu, and Julien Arné. 2018. Learning to Recognize Touch Gestures: Recurrent vs. Convolutional Features and Dynamic Sampling. In *FG'2018-13th IEEE International Conference on Automatic Face and Gesture Recognition*. 114–121.
- [10] Alexey Dosovitskiy, Lucas Beyer, Alexander Kolesnikov, Dirk Weissenborn, Xiaohua Zhai, Thomas Unterthiner, Mostafa Dehghani, Matthias Minderer, Georg Heigold, Sylvain Gelly, et al. 2020. An Image is Worth 16x16 Words: Transformers

- for Image Recognition at Scale. In *International Conference on Learning Representations*.
- [11] Mohamed W Abo El-Soud, Tarek Gaber, Fayez Alfayez, and Mohamed Meselhy Eltoukhy. 2021. Implicit authentication method for smartphone users based on rank aggregation and random forest. *Alexandria Engineering Journal* 60, 1 (2021), 273–283.
 - [12] Giacomo Giorgi, Andrea Saracino, and Fabio Martinelli. 2021. Using recurrent neural networks for continuous authentication through gait analysis. *Pattern Recognition Letters* 147 (2021), 157–163.
 - [13] Kai Han, An Xiao, Enhua Wu, Jianyuan Guo, Chunjing Xu, and Yunhe Wang. 2021. Transformer in transformer. *Advances in Neural Information Processing Systems* 34 (2021).
 - [14] Kaiming He, Xiangyu Zhang, Shaoqing Ren, and Jian Sun. 2016. Deep residual learning for image recognition. In *Proceedings of the IEEE conference on computer vision and pattern recognition*. 770–778.
 - [15] Luis Hernández-Álvarez, José María De Fuentes, Lorena González-Manzano, and Luis Hernández Encinas. 2021. SmartCAMPP-Smartphone-based continuous authentication leveraging motion sensors with privacy preservation. *Pattern Recognition Letters* 147 (2021), 189–196.
 - [16] IDNet dataset. [n. d.]. <http://signalnet.dei.unipd.it/research/human-sensing/>, IDNet dataset (Ed.).
 - [17] Yifan Jiang, Shiyu Chang, and Zhangyang Wang. 2021. Transgan: Two pure transformers can make one strong gan, and that can scale up. *Advances in Neural Information Processing Systems* 34 (2021).
 - [18] Sowndarya Krishnamoorthy, Luis Rueda, Sherif Saad, and Haytham Elmiligi. 2018. Identification of user behavioral biometrics for authentication using keystroke dynamics and machine learning. In *Proceedings of the 2018 2nd International Conference on Biometric Engineering and Applications*. 50–57.
 - [19] Shaohua Li, Xiuchao Sui, Xiangde Luo, Xinxing Xu, Yong Liu, and Rick Siow Mong Goh. 2021. Medical Image Segmentation using Squeeze-and-Expansion Transformers. In *IJCAI*.
 - [20] Yantao Li, Hailong Hu, and Gang Zhou. 2018. Using data augmentation in continuous authentication on smartphones. *IEEE Internet of Things Journal* 6, 1 (2018), 628–640.
 - [21] Yantao Li, Hailong Hu, Zhangqian Zhu, and Gang Zhou. 2020. SCANet: sensor-based continuous authentication with two-stream convolutional neural networks. *ACM Transactions on Sensor Networks (TOSN)* 16, 3 (2020), 1–27.
 - [22] Yantao Li, Jiaxing Luo, Shaojiang Deng, and Gang Zhou. 2021. CNN-based Continuous Authentication on Smartphones with Conditional Wasserstein Generative Adversarial Network. *IEEE Internet of Things Journal* (2021).
 - [23] Yantao Li, Peng Tao, Shaojiang Deng, and Gang Zhou. 2021. DeFFusion: CNN-based Continuous Authentication Using Deep Feature Fusion. *ACM Transactions on Sensor Networks (TOSN)* 18, 2 (2021), 1–20.
 - [24] Yehao Li, Ting Yao, Yingwei Pan, and Tao Mei. 2022. Contextual transformer networks for visual recognition. *IEEE Transactions on Pattern Analysis and Machine Intelligence* (2022).
 - [25] Ze Liu, Yutong Lin, Yue Cao, Han Hu, Yixuan Wei, Zheng Zhang, Stephen Lin, and Baining Guo. 2021. Swin transformer: Hierarchical vision transformer using shifted windows. In *Proceedings of the IEEE/CVF International Conference on Computer Vision*. 10012–10022.
 - [26] Michail D Papamichail, Kyriakos C Chatzidimitriou, Thomas Karanikiotis, Napoleon-Christos I Oikonomou, Andreas L Symeonidis, and Sashi K Saripalle. 2019. Brainrun: A behavioral biometrics dataset towards continuous implicit authentication. *Data* 4, 2 (2019), 60.
 - [27] Stanislav Pidhorskyi, Ranya Almohsen, and Gianfranco Doretto. 2018. Generative probabilistic novelty detection with adversarial autoencoders. *Advances in neural information processing systems* 31 (2018).
 - [28] Prajit Ramachandran, Niki Parmar, Ashish Vaswani, Irwan Bello, Anselm Levskaya, and Jon Shlens. 2019. Stand-alone self-attention in vision models. *Advances in Neural Information Processing Systems* 32 (2019).
 - [29] Aditi Roy, Tzipora Halevi, and Nasir Memon. 2015. An HMM-based multi-sensor approach for continuous mobile authentication. In *MILCOM 2015-2015 IEEE Military Communications Conference*. IEEE, 1311–1316.
 - [30] Chao Shen, Yuanxun Li, Yufei Chen, Xiaohong Guan, and Roy A Maxion. 2017. Performance analysis of multi-motion sensor behavior for active smartphone authentication. *IEEE Transactions on Information Forensics and Security* 13, 1 (2017), 48–62.
 - [31] Chao Shen, Yong Zhang, Xiaohong Guan, and Roy A Maxion. 2016. Performance Analysis of Touch-Interaction Behavior for Active Smartphone Authentication. *IEEE Transactions on Information Forensics and Security* 3, 11 (2016), 498–513.
 - [32] Zhihao Shen, Shun Li, Xi Zhao, and Jianhua Zou. 2022. MMAAuth: A Continuous Authentication Framework on Smartphones Using Multiple Modalities. *IEEE Transactions on Information Forensics and Security* 17 (2022), 1450–1465.
 - [33] Devu Manikantan Shila and Emeka Eyisi. 2018. Adversarial gait detection on mobile devices using recurrent neural networks. In *2018 17th IEEE International Conference on Trust, Security and Privacy in Computing and Communications/12th IEEE International Conference on Big Data Science and Engineering (TrustCom/BigDataSE)*. IEEE, 316–321.
 - [34] Zdenka Sitova, Jaroslav Sedenka, Qing Yang, Ge Peng, Gang Zhou, Paolo Gasti, and Kiran S Balagani. 2016. HMOG: New Behavioral Biometric Features for Continuous Authentication of Smartphone Users. *IEEE Transactions on Information Forensics and Security* 11, 5 (2016), 877–892.

- [35] Ioannis Stylios, Spyros Kokolakis, Olga Thanou, and Sotirios Chatzis. 2021. Behavioral biometrics & continuous user authentication on mobile devices: A survey. *Information Fusion* 66 (2021), 76–99.
- [36] Alaa Tharwat, Abdelhameed Ibrahim, Tarek Gaber, and Aboul Ella Hassanien. 2018. Personal identification based on mobile-based keystroke dynamics. In *International Conference on Advanced Intelligent Systems and Informatics*. Springer, 457–466.
- [37] Ashish Vaswani, Noam Shazeer, Niki Parmar, Jakob Uszkoreit, Llion Jones, Aidan N Gomez, Lukasz Kaiser, and Illia Polosukhin. 2017. Attention is all you need. *Advances in neural information processing systems* 30 (2017).
- [38] Pascal Vincent, Hugo Larochelle, Yoshua Bengio, and Pierre-Antoine Manzagol. 2008. Extracting and composing robust features with denoising autoencoders. In *Proceedings of the 25th international conference on Machine learning*. 1096–1103.
- [39] Cong Wang, Yanru Xiao, Xing Gao, Li Li, and Jun Wang. 2021. A Framework for Behavioral Biometric Authentication using Deep Metric Learning on Mobile Devices. *IEEE Transactions on Mobile Computing* (2021).
- [40] Yujing Wang, Yaming Yang, Jiangan Bai, Mingliang Zhang, Jing Bai, Jing Yu, Ce Zhang, Gao Huang, and Yunhai Tong. 2021. Evolving attention with residual convolutions. In *International Conference on Machine Learning*. PMLR, 10971–10980.
- [41] Haiping Wu, Bin Xiao, Noel Codella, Mengchen Liu, Xiyang Dai, Lu Yuan, and Lei Zhang. 2021. Cvt: Introducing convolutions to vision transformers. In *Proceedings of the IEEE/CVF International Conference on Computer Vision*. 22–31.
- [42] Lei Yang, Yi Guo, Xuan Ding, Jinsong Han, Yunhao Liu, Cheng Wang, and Changwei Hu. 2015. Unlocking Smart Phone through Handwaving Biometrics. *IEEE Transactions on Mobile Computing* 5, 14 (2015), 1044–1055.
- [43] Yafang Yang, Bin Guo, Zhu Wang, Mingyang Li, Zhiwen Yu, and Xingshe Zhou. 2019. BehaveSense: Continuous authentication for security-sensitive mobile apps using behavioral biometrics. *Ad Hoc Networks* 84 (2019), 9–18.
- [44] Yingyuan Yang, Jinyuan Sun, and Linke Guo. 2019. PersonaIA: A Lightweight Implicit Authentication System Based on Customized User Behavior Selection. *IEEE Transactions on Dependable and Secure Computing* 16, 1 (2019), 113–126.
- [45] Hongbo Zhang, Chungang Yan, Peihai Zhao, and Mimi Wang. 2016. Model construction and authentication algorithm of virtual keystroke dynamics for smart phone users. In *2016 IEEE International Conference on Systems, Man, and Cybernetics (SMC)*. IEEE, 000171–000175.
- [46] Tiantian Zhu, Zhengqiu Weng, Guolang Chen, and Lei Fu. 2020. A hybrid deep learning system for real-world mobile user authentication using motion sensors. *Sensors* 20, 14 (2020), 3876.
- [47] Tiantian Zhu, Zhengqiu Weng, Qijie Song, Yuan Chen, Qiang Liu, Yan Chen, Mingqi Lv, and Tieming Chen. 2020. ES-PIALCOG: General, Efficient and Robust Mobile User Implicit Authentication in Noisy Environment. *IEEE Transactions on Mobile Computing* (2020).
- [48] Qin Zou, Yanling Wang, Qian Wang, Yi Zhao, and Qingquan Li. 2020. Deep learning-based gait recognition using smartphones in the wild. *IEEE Transactions on Information Forensics and Security* 15 (2020), 3197–3212.